Journal of Assisted Reproduction and Genetics (2019) 36:857–873
https://doi.org/10.1007/s10815-019-01442-9

REPRODUCTIVE PHYSIOLOGY AND DISEASE

Transcriptomic analysis of the interaction of choriocarcinoma spheroids with receptive vs. non-receptive endometrial epithelium cell lines: an in vitro model for human implantation

Paula Vergaro[1,2] · Gustavo Tiscornia[1,3] · Amelia Rodríguez[1] · Josep Santaló[2] · Rita Vassena[1]

Received: 11 January 2019 / Accepted: 19 March 2019 / Published online: 10 April 2019

Abstract

Purpose Several in vitro systems have been reported to model human implantation; however, the molecular dynamics of the trophoblast vs. the epithelial substrate during attachment have not been described. We have established an in vitro model which allowed us to dissect the transcriptional responses of the trophoblast and the receptive vs. non-receptive epithelium after co-culture.

Methods We established an in vitro system based on co-culture of (a) immortalized cells representing receptive (Ishikawa) or non-receptive (HEC-1-A) endometrial epithelium with (b) spheroids of a trophoblastic cell line (JEG-3) modified to express green fluorescent protein (GFP). After 48 h of co-culture, GFP+ (trophoblast cells) and GFP− cell fractions (receptive or non-receptive epithelial cells) were isolated by fluorescence-activated flow cytometry (FACS) and subjected to RNA-seq profiling and gene set enrichment analysis (GSEA).

Results Compared to HEC-1-A, the trophoblast challenge to Ishikawa cells differentially regulated the expression of 495 genes, which mainly involved cell adhesion and extracellular matrix (ECM) molecules. GSEA revealed enrichment of pathways related to cell division, cell cycle regulation, and metabolism in the Ishikawa substrate. Comparing the gene expression profile of trophoblast spheroids revealed that 1877 and 323 genes were upregulated or downregulated when co-cultured on Ishikawa substrates (compared to HEC-1-A), respectively. Pathways favorable to development, including tissue remodeling, organogenesis, and angiogenesis, were enhanced in the trophoblast compartment after co-culture of spheroids with receptive epithelium. By contrast, the co-culture with less receptive epithelium enriched pathways mainly related to trophoblast cell proliferation and cell cycle regulation.

Conclusions Endometrial receptivity requires a transcriptional signature that determines the trophoblast response and drives attachment.

Keywords Implantation · Attachment · Endometrial receptivity · Transcriptomics

Introduction

Despite the efforts to develop in vivo and in vitro approaches to study human implantation, the molecular mechanisms directing this process are still poorly understood. Successful implantation requires a highly orchestrated process dependent on correct coordination of the molecular crosstalk between the different cellular compartments involved, namely, the trophoblast, and both the epithelium and the stroma of the endometrium [1]. The initial interaction between the embryo and the epithelium is supported by molecules secreted from both compartments into the uterine fluid [2–4]. Initially, the blastocyst establishes a reversible first contact with the luminal epithelial surface (apposition). This is followed by the establishment of

Electronic supplementary material The online version of this article (https://doi.org/10.1007/s10815-019-01442-9) contains supplementary material, which is available to authorized users.

✉ Rita Vassena
rvassena@eugin.es

[1] Clínica EUGIN, Travessera de les Corts 322, 08029 Barcelona, Spain

[2] Facultat de Biociències, Departament de Biologia Cel·lular, de Fisiologia i d'Immunologia, Universitat Autònoma de Barcelona, Barcelona, Spain

[3] Centro de Investigação em Biomedicina (CBMR), Universidade do Algarve, Faro, Portugal

a stronger, irreversible interaction (attachment). After the initial interaction with, and breaching of, the luminal epithelium, the trophoblast must invade the underlying stromal compartment to establish a pregnancy [5]. Studies focused on the stroma have highlighted its relevance to the implantation success; this is mainly due to the unique activity of decidualized cells, which act as a biosensor of embryo quality and trigger a transient pro-inflammatory response linked to endometrial receptivity [6–8]. How these processes are controlled in the cycling endometrium is still unknown, although it has been proposed that uterine NK cells and the decidualization-associated senescence in endometrial tissue are responsible for endometrial receptivity and remodeling [9]. Knowledge of the molecular mechanisms governing the initial attachment of the embryo to the epithelial surface is more limited. Using an in vitro model for attachment between mouse blastocysts and carcinoma-derived epithelial cells, Ruane et al. have demonstrated that endometrial molecular signals critically regulate the trophoblast differentiation needed for breaching and invasion [10].

The study of implantation is essential to understand and characterize implantation failure, a frequent cause of human infertility [11]. Impaired endometrial receptivity is an important limiting factor of IVF success when high-quality embryos are transferred [12]. Since it is not possible to study implantation in vivo, the biological mechanisms underpinning this process are difficult to access; further, in vitro assays are hampered by low availability of human embryos and fresh endometrial tissue to establish primary cultures. A number of publications have approached the study of implantation using knock-out mice models (as reviewed in [13]). However, the mechanistic details of implantation are species-specific and limit the usefulness of mice studies to describe human implantation [5, 14]. In particular, the rapid sequence of implantation events and the differences with the human mechanisms of attachment, invasion, and placentation do not make the mouse a good model for studying early implantation [14–16]. A common approach to overcome these limitations is the use of cell lines. The epithelial cell lines Ishikawa (receptive) and HEC-1-A (minimally receptive) have been widely used to model different aspects of human implantation due to their differential response to embryo attachment [17–21]. In vitro systems have allowed the study of different stages of implantation by co-culturing both compartments to detect specific molecules at the mRNA transcript or protein levels [20, 22], to test the effect of candidate drugs [19, 23, 24] or to describe morphological changes during implantation [25]. Importantly, most in vitro approaches employed to date analyze the response of the whole co-culture system, without dissecting the response of each compartment. To overcome this limitation, we have devised a system to dissect the transcriptional dynamics of the trophoblast and the epithelium during the attachment and initial invasion. Using the cell line JEG-3 as a proxy for the trophoblast, and the cell lines Ishikawa and HEC-1-A as receptive and non-receptive endometrial epithelia, respectively, our in vitro model allows for an efficient separation of both compartments by fluorescence-activated cell sorting (FACS). Through RNA-seq transcriptomic analysis, we quantified the transcriptional changes occurring in the trophoblast and the epithelium (receptive vs. minimally receptive) after 48 h of co-culture in a 2-D in vitro system.

Materials and methods

Cell culture

The human endometrial adenocarcinoma cell lines Ishikawa (ECACC 99040201) and HEC-1-A (ATCC HTB-112) and the human trophoblast choriocarcinoma cell line JEG-3 (ATCC HTB-36) were cultured as indicated by the provider. Ishikawa cells were maintained in MEM (MEM α, nucleosides, no phenol red) supplemented with 5% fetal bovine serum, 10 mM of non-essential amino acids (MEM Non-Essential Amino Acids Solution), and 100 mg/ml streptomycin and 100 IU/ml penicillin (PenStrep). HEC-1-A were maintained in McCoy's 5A (McCoy's 5A (Modified) Medium, GlutaMAX™ Supplement) supplemented with 10% fetal bovine serum and 100 mg/ml streptomycin and 100 IU/ml penicillin (PenStrep). JEG-3 cells were cultured in DMEM (DMEM, high glucose, GlutaMAX™ supplement) containing 10% fetal bovine serum, 1 mM sodium pyruvate, and 100 mg/ml streptomycin and 100 IU/ml penicillin (PenStrep). All cell lines were kept at 37 °C and media was changed every other day. Unless otherwise indicated, all reagents were purchased from Gibco, Thermo Fisher Scientific, USA.

Generation of fluorescent JEG-3 spheroids

Recombinant lentiviral particles (third-generation self-inactivating vector system) expressing green fluorescent protein (GFP) from a PGK promoter were produced as described [26] and used to transduce the JEG-3 trophoblast cells. Briefly, trophoblast cells were plated on 12-well plates and cultured to 70% confluence. Aliquots of lentiviral particles were diluted to achieve an estimated multiplicity of infection (MOI) of 10 in a final volume of 500 μl. After 24 h, cells were rinsed with Dulbecco's phosphate-buffered saline (DPBS without calcium or magnesium) and fresh medium was added. Cells were cultured and passaged three times to avoid lentivirus carryover. Trophoblast cells with the highest GFP levels were sorted and collected for further culture by fluorescence-activated cell sorting (FACS). Cell suspensions of GFP-positive JEG-3 cells were diluted to a final concentration of 3×10^4 cells/ml. One hundred microliters of the cell

suspension (3000 cells) were seeded in U-bottom ultra-low attachment 96-well plates (Corning, NY, USA). Plates were centrifuged at room temperature during 10 min at 250×*g* and cultured for 48 h at 37 °C and 5% CO_2 generating fluorescent spheroids of 250–300 μM (10,000 cells).

In vitro attachment assay

An in vitro model of implantation was established to mimic the molecular changes during attachment and initial invasion. The cell line Ishikawa was used as a model of receptive epithelium, while the cell line HEC-1-A represented the non-receptive epithelium. Both Ishikawa and HEC-1-A were cultured in 96-well plates (Nunc, Thermo Fisher Scientific, USA) until the cells reached confluence. GFP-positive JEG-3 spheroids formed by around 10,000 cells were added to each 96-well (one spheroid per well). Our experimental design (see Fig. 1) used pools of small wells containing a single spheroid to increase trophoblast to epithelium ratio, and optimize the detection of transcriptional changes induced by the interaction in those areas of the substrate far from the spheroid. Co-cultures were maintained for 48 h in 1:1 mix of MEM/DMEM in case of the Ishikawa-JEG-3 co-culture and 1:1 mix of McCoy's 5A/DMEM in case of the HEC-1-A-JEG-3 co-culture. In parallel, 96-well plates of confluent Ishikawa, HEC-1-A, and JEG-3 spheroids cultured without addition of any other cell type for 48 h were used as experimental controls for the effect of time of co-culture. After 48 h, all the monocultures and co-cultures were washed with DPBS and cells were harvested from the 96-well plates using TrypLE™ Express Enzyme and pooled before cell sorting. All reagents were purchased from Gibco, Thermo Fisher Scientific, USA. Co-culture experiments were performed three times as independent biological triplicates.

Cell sorting and RNA extraction

FACS (BD FACS Aria Fusion II cell sorter, BD Biosciences, USA) was used to separate GFP-positive trophoblast cells from unlabeled epithelial substrates after co-culture. The following cell fractions were collected: Ishikawa control (I-c), HEC-1-A control (H-c), JEG-3 spheroids control (S-c), Ishikawa substrates co-cultured with JEG-3 spheroids (I-co-S), HEC-1-A substrates co-cultured with JEG-3 spheroids (H-co-S), JEG-3 spheroids co-cultured with Ishikawa substrates (S-co-I), and JEG-3 spheroids co-cultured with HEC-1-A substrates (S-co-H) (Fig. 1). To minimize RNA degradation, all handling procedures were performed on ice; the cytometer

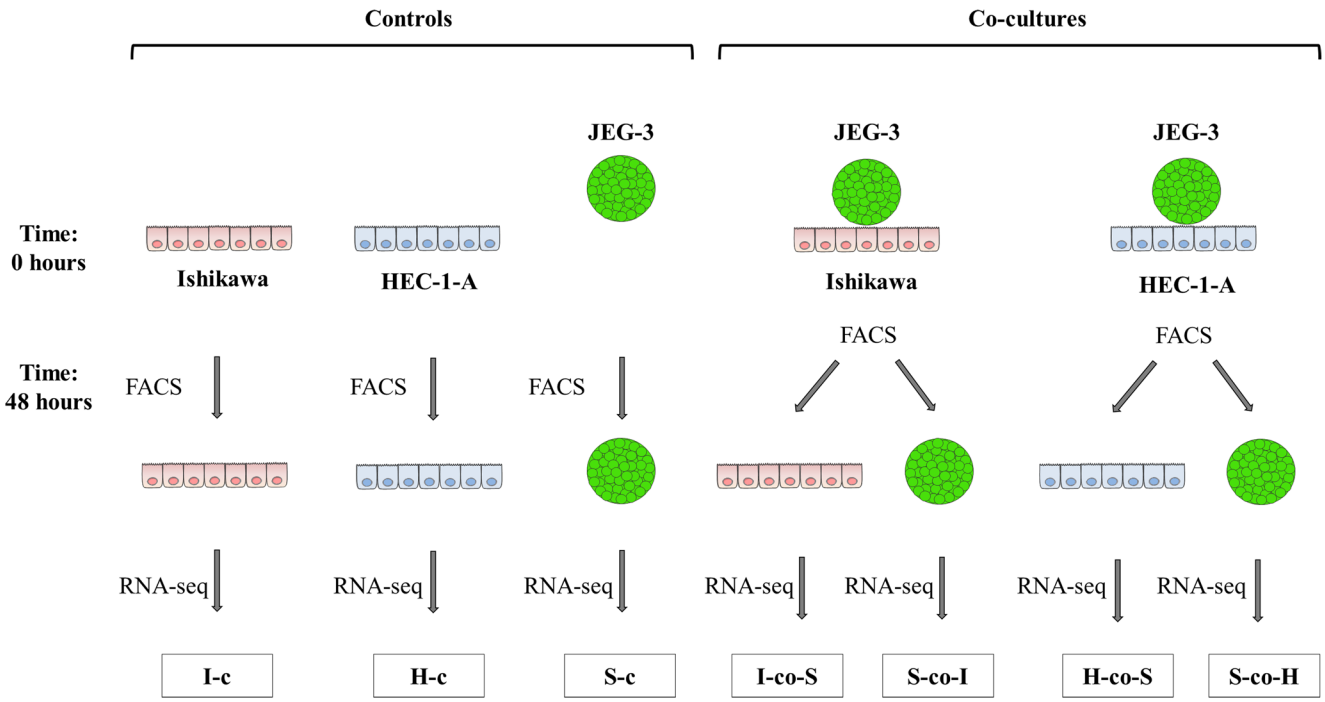

Fig. 1 Scheme of the experimental design; monolayers of receptive (Ishikawa) and non-receptive (HEC-1-A) epithelia were co-cultured with trophoblast spheroids (JEG-3) for 48 h, or maintained in monocultures for the same time as controls. Likewise, single spheroids were co-cultured or cultured for 48 h in absence of any substrate as controls. All the JEG-3 spheroids depicted express GFP. After 48 h, GFP+ (trophoblast) and GFP− (receptive or non-receptive epithelia) were separated by FACS and analyzed by RNA-seq. The transcriptomic profiles of the following cell fractions were obtained: Ishikawa control (I-c), HEC-1-A control (H-c), JEG-3 spheroids control (S-c), Ishikawa substrates co-cultured with JEG-3 spheroids (I-co-S), HEC-1-A substrates co-cultured with JEG-3 spheroids (H-co-S), JEG-3 spheroids co-cultured with Ishikawa substrates (S-co-I), and JEG-3 spheroids co-cultured with HEC-1-A substrates (S-co-H)

chamber was cooled to 4 °C before cell sorting. Cell suspensions were filtered through a 70-μm mesh to eliminate cellular aggregates before sorting. One hundred micrometer sorter nozzles were used to minimize clog formation during cell sorting. Dead cells were identified by diamidino-2-phenylindole (DAPI) staining and excluded from the sorted populations. GFP-positive and GFP-negative fractions were collected in 50 μl of DPBS without calcium or magnesium on ice, centrifuged and cell pellets were stored at − 20 °C until processed. RNA from each fraction of the three independent experiments was isolated using the RNeasy Mini Kit (Qiagen N. V., Netherlands) following the manufacturer's recommendations and eluted in 30 μl nuclease-free water. RNA was purified using RNase-Free DNase Set (Qiagen N. V., Netherlands) and concentration was measured by fluorometric quantitation (QuBit, Thermo Fisher Scientific, USA). RNA integrity number (RIN) was 8.5 to 10 in all samples as determined by Bioanalyzer 2100 System (Agilent Technologies, USA).

cDNA library preparation and RNA-seq

A total of 21 RNA samples (3 replicates of each of the 7 experimental cell populations) were used for cDNA library preparation and RNA-seq analysis.

After performing the quality control of the 21 samples, polyA mRNA was isolated using NEBNext Poly(A) mRNA Magnetic Isolation Module (https://www.neb.com/products/e7490-nebnext-polya-mrna-magnetic-isolation-module#Product%20Information) following the manufacturer's instructions. Once mRNA was purified, cDNA generation, End repair, and Ligate Adaptor for Illumina were done using the kit NEBNext Ultra II RNA Library Prep for Illumina following the manufacturer's instructions. Samples were amplified with SYBR green to establish the minimum number of cycles required. During the amplification, each sample was labeled with a specific barcode using the NEBNext Multiplex Oligos kit for Illumina (Index Primers Set 1). Finally, three equimolar 7 sample pools were generated, and each pool was sequenced in a single 50 nt Single Read lane of an Illumina Hiseq 2500 system, getting more than 30 million reads per sample.

RNA-seq data analysis

Reads were aligned to the hg19 version of the human genome with the STAR software v2.3.0e [27] and default parameters. The aligned reads were binarized and sorted with sambamba v0.5.9 (http://lomereiter.github.io/sambamba/). Reads were imported to R (https://www.R-project.org/) with the inbuilt annotation in the Rsubread package [28]. Further annotations were downloaded from Biomart [29] using the corresponding R package.

Differential expression was performed with DESeq2 [30] with processing batch as covariate.

Enrichment analysis

Pathway enrichment was assessed through the pre-ranked version of Gene Set Enrichment Analysis (GSEA) [31]. GSEA was applied to the ranking defined by the log2 fold change (log2FC) of the differential expression analysis using DESeq2. Gene sets for analyses belonged to the Gene Ontology (GO) [32] terms as collected in the GSEABase R package [33], or to the Hallmark collection [34] after retrieval from the MsigDB [35]. The significance cutoff for false discovery rate (FDR) was set at 0.01.

In order to assess the enrichment of genes showing significant interaction between HEC-1-A and Ishikawa when comparing co-cultured and non-co-cultured control fractions, we categorized genes with adjusted p value for the interaction lower than 0.05 in the following four groups: larger effect (either positive or negative) in HEC-1-A than in Ishikawa (absolute value of the size estimate in Ishikawa lower than 0.25 and size estimate higher (lower) than 0.75 (− 0.75)) in HEC-1-A. Larger effect (either positive or negative) in Ishikawa than in HEC-1-A (absolute value of the size estimate in HEC-1-A lower than 0.25 and size estimate higher (lower) than 0.75 (− 0.75)) in Ishikawa. We tested enrichment of these gene signatures in the Gene Ontology collections [32] and the Hallmarks gene sets from the Broad Institute [35]. Gene sets were filtered for sizes larger than 10 and smaller than 2000. We used a hypergeometric test for statistical significance with Benjamin-Hochberg adjustment for multiple testing.

Statistical analysis

Linear regression and pairwise comparison were used to analyze differential gene expression between cell populations sorted by FACS. Statistical significance was set at an absolute log2 fold change (log2FC) ≥ 1 and a q value of < 0.05 (adjusted p value < 0.05 with Benjamin-Hochberg correction for multiple comparisons).

RNA-seq validation by qPCR

A molecular quantitative analysis was performed to confirm the expression patterns of selected genes among the same samples used in the RNA-seq. The validation was performed using 5 ng (in triplicate) of the cDNA libraries previously constructed in a final volume of 20 μl. Gene expressions were quantified using 2× SsoAdvanced Universal SYBR Green Supermix (Bio-Rad, Hercules, CA, USA) on a CFX Real-Time PCR platform (Bio-Rad, Hercules, CA, USA). The selected genes and their forward and reverse primer sequences

(5′–3′) were the following: *TMEM255A* (ACCTGCTT CTGCTGTGACCT and TCTTGGCAACTGCTGACATC), *EREG* (CACAGTCGTCGGTTCCAC and CTCTGGAT CCCCTGAGGT), *SPDYC* (TCAGCCTTCTGGAG GACAGT and CACCATGGCCAGGAGATACT), *CYP19A1* (GTGGACGTGTTGACCCTTCT and CACGATAGCACTTTCGTCCA), *CASC1* (GGTGGGAT GCTGAAGGTAAA and AAAGGTGTCCAGGCTGAATG), *PROM1* (GCCACCGCTCTAGATACTGC and GCTTTTCCTATGCCAAACCA), *TGFA* (TTCCCACA CTCAGTTCTGCTT and ACGTACCCAGAATGGCAGAC), *CDC20B* (GTAGTTGGGGCTCTGAGCTG and GGCTACCCGAACATCGTG), and *HPRT1* (TGACACTG GCAAAACAATGCA and GGTCCTTTTCACCA GCAAGCT). The final products were analyzed using the CFX Manager Software (Bio-Rad, Hercules, CA, USA). To select the most stable normalizers, the Integrated Cotton EST Database was used [36]; *MAP4K4* and *TBP* were used as housekeeping genes, using the following forward and reverse primer sequences (5′–3′): CTTGGATGGTGTGTTCATGC and AGACCGAACAGAGGCAAAGA for *MAP4K4* and TATAATCCCAAGCGGTTTGC and GCTGGAAA ACCCAACTTCTG for *TBP*. Gene expression data were calculated as the ratios between the gene expression values of the selected genes and the geometric average of *MAP4K4* and *TBP* expressions [37]. Amplification specificity was confirmed by analyzing the qPCR melting curves of the final products.

Results

Transcriptional changes induced by trophoblast-epithelium interaction

After 48 h of co-culture, the spheroids attached firmly to the Ishikawa cells, flattened out, and expanded radially on the substrate (Fig. 2a). In contrast, after the interaction with the minimally receptive HEC-1-A cells, the trophoblast spheroids adhered to the monolayer but did not expand onto the substrate cells (Fig. 2b). After co-culture, trophoblast and epithelial compartments (receptive Ishikawa or minimally receptive HEC-1-A) were isolated by FACS. The transcriptional changes of the sorted cell populations were individually analyzed by comprehensive RNA-seq profiling. GFP-positive fractions corresponded to the co-cultured JEG-3 trophoblast spheroids or controls, while GFP-negative cell populations corresponded to co-cultured Ishikawa or HEC-1-A, or their respective controls. RNA-seq data are available in the public database Gene Expression Omnibus (GEO) repository (accession GSE121790).

Sample clustering and quality control

Principal component analysis (PCA) was used to identify sample clustering and possible technical bias between experimental triplicates (Supplementary Fig. 1). PCA clearly revealed distinctive expression patterns among sorted cell populations and clustering of experimental triplicates by sample group; First and second components (PC1 and PC2) accounted for 52.5 and 36.0% of sample variability, respectively.

Transcriptional dynamics of the epithelial substrates

Pairwise comparisons of transcriptome dynamics in both trophoblast spheroids and epithelial compartments were performed. In each of the three experimental replicates, a total of seven gene expression datasets were generated from the cell fractions collected by FACS, including trophoblast or epithelial fractions after co-culture and their correspondent non-co-cultured controls, as described in the "Materials and methods" section and Fig. 1. We found striking differences in gene expression profiles when comparing the control receptive vs. control non-receptive substrates: as many as 6628 genes were differentially expressed between I-c and H-c (3957 genes upregulated and 2671 downregulated in I-c as compared to H-c, respectively; Fig. 3a, Supplementary File S1). After co-culture with spheroids (I-co-S), the receptive substrate (Ishikawa), showed 608 differentially expressed genes (as compared to I-c), of which 310 genes were upregulated and 298 genes downregulated (Fig. 3b, Supplementary File S2). The top 10 differentially expressed genes of this set (ranked by absolute log2FC) are listed in Fig. 4. Interestingly, the comparison between H-co-S and H-c yielded only nine differentially expressed genes (five genes upregulated and four genes downregulated in H-co-S, respectively; Fig. 3c, Supplementary File S3). Three of these genes were also present in I-co-S vs. I-c dataset (*SYNGR3*, *CYP1A1*, and *ANK1*) (Fig. 4). Co-cultured epithelial Ishikawa and HEC-1-A substrates could not be compared directly, as their respective controls were different cell lines; however, when we performed an analysis of differential expression patterns between I-co-S and I-c as compared to the differential expression patterns between H-co-S and H-c, we found 495 genes which changed their expression patterns among both interaction pairs (Supplementary File S4).

Transcriptional dynamics of the trophoblast spheroids

Comparison of transcriptome dynamics in the trophoblast compartment after co-culture on Ishikawa (S-co-I) showed

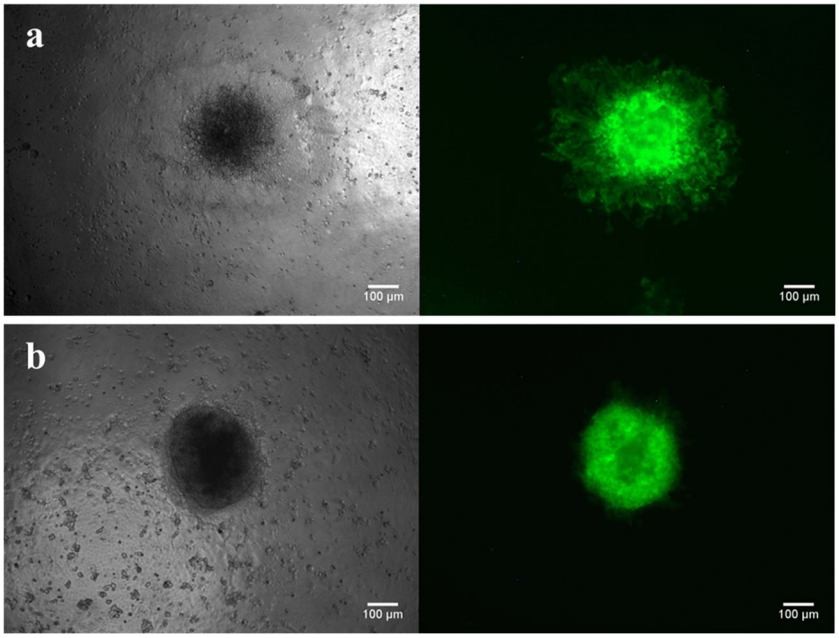

Fig. 2 Representative figures of GFP+ trophoblast spheroids attached to Ishikawa (**a**) and adhered to HEC-1-A (**b**) monolayers after 48 h co-culture, visualized under × 10 magnification

important differential gene expression when compared to non-co-cultured control (S-c): a total of 3976 genes were differentially expressed between S-co-I and S-c (3220 genes upregulated and 756 genes downregulated in S-co-I compared to S-c, respectively; Fig. 3d, Supplementary File S5). Interestingly, fewer genes significantly changed their expression levels when the transcriptomic profile of S-co-H was compared with that of S-c (only 1038 genes showed differential expression, with 949 genes upregulated and 89 genes downregulated, respectively; Fig. 3e, Supplementary File S6).

A direct comparison of JEG-3 spheroids after co-culture on Ishikawa or HEC-1-A (S-co-I vs. S-co-H), possibly due to the fact that both compartments have the same control (S-c), showed 2200 differentially expressed genes (1877 genes upregulated and 323 genes downregulated in S-co-I vs. S-co-H, respectively; Fig. 3f, Supplementary File S7). Some of these genes were also differentially expressed in I-co-S vs. I-c comparison (209, listed in Supplementary File S8, of which the top 10 differentially expressed genes are shown in Fig. 4), and only two genes (*CYP1A1* and *TACSTD2*) were differentially expressed in H-co-S vs. H-c (Fig. 4).

Enrichment analysis of the epithelial substrates

GSEA was applied to all gene set comparisons to reveal the biological pathways enriched in each group. Gene ontology biological process (GOBP) and Broad Hallmarks annotations were used to classify functionally related genes overrepresented in co-cultured GFP+ and GFP− cell fractions. Biological pathways overrepresented in each gene set comparison are showed in Tables 1, 2, 3, 4, and 5. Compared to I-c, the pathways enriched in I-co-S were mostly related to spindle organization and cell cycle regulation (e.g., mitotic spindle organization, E2F targets, and G2M checkpoint) (Table 1). In contrast, only one pathway was significantly enriched in the comparison H-co-S vs. H-c (regulation of amino acid transport) (Table 2). A hypergeometric test was used to perform gene enrichment analysis of epithelial substrates in both interactions (I-co-S and I-c vs. H-co-S and H-c). Of the four gene expression patterns included in this test, only one achieved statistical significance; it included those genes which were upregulated in I-co-S vs. I-c and downregulated or unchanged in H-co-S vs. H-c (Table 3). The results suggested that the transcriptional changes in the receptive and non-receptive epithelium after the trophoblast challenge mainly involved pathways related to cell division and cell cycle regulation (e.g., nuclear division, chromosome segregation, and metaphase/anaphase transition of mitotic cell cycle) as well as metabolism (i.e., cholesterol biosynthetic process, sterol biosynthetic process, and cholesterol homeostasis).

Fig. 3 Volcano plots of differentially expressed genes between co-cultured and sorted GFP+ and GFP− cell fractions as well as non-co-cultured controls in pairwise comparisons: **a** Ishikawa control (I-c) vs. HEC-1-A control (H-c), **b** Ishikawa substrates co-cultured with JEG-3 spheroids (I-co-S) vs. Ishikawa control (I-c), **c** HEC-1-A substrates co-cultured with JEG-3 spheroids (H-co-S) vs. HEC-1-A control (H-c), **d** JEG-3 spheroids co-cultured with Ishikawa substrates (S-co-I) vs. JEG-3 spheroids control (S-c), **e** JEG-3 spheroids co-cultured with HEC-1-A substrates (S-co-H) vs. JEG-3 spheroids control (S-c), and **f** JEG-3 spheroids co-cultured with Ishikawa substrates (S-co-I) vs. JEG-3 spheroids co-cultured with HEC-1-A substrates (S-co-H) ▶

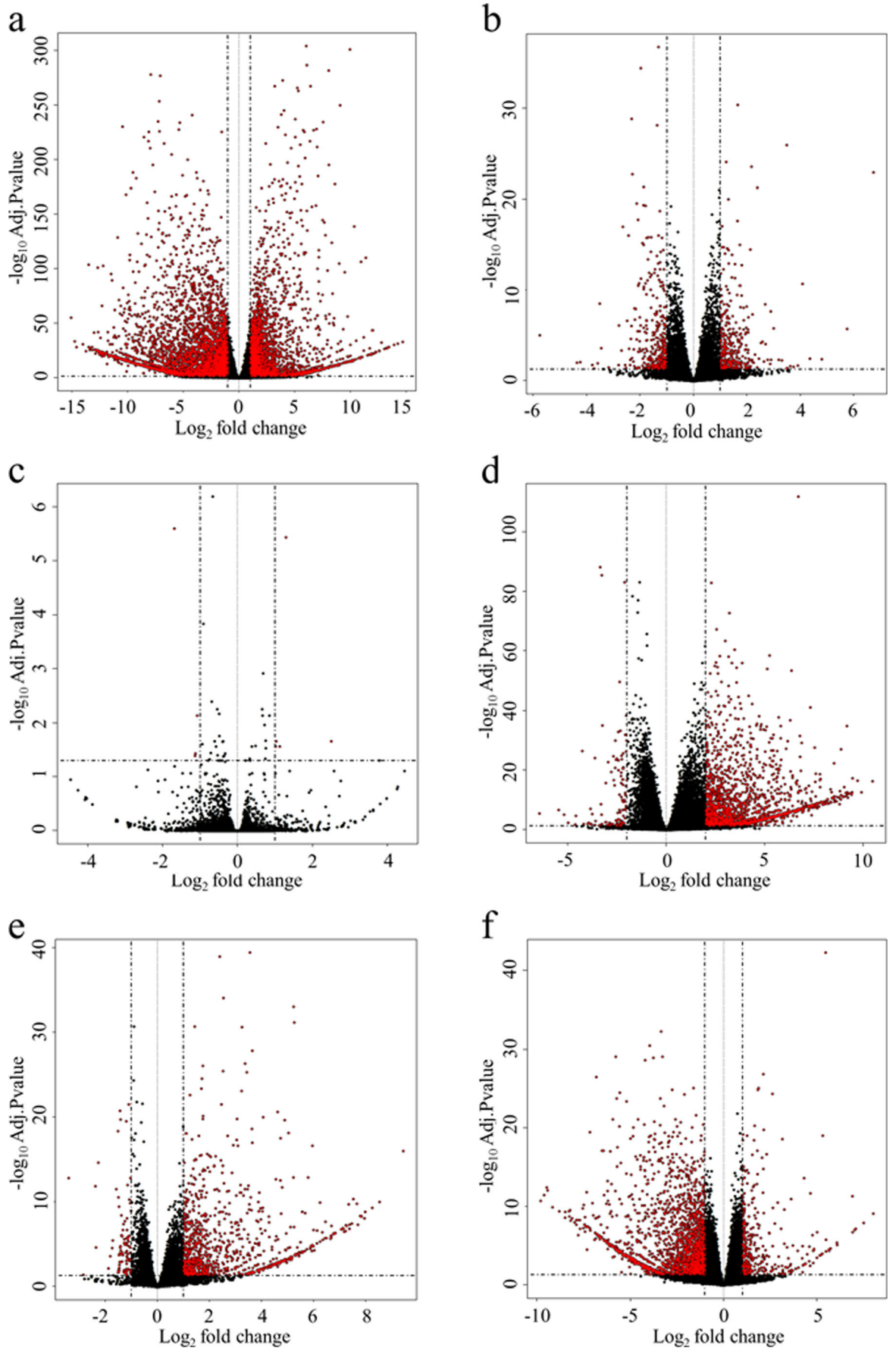
a
-log10 Adj.Pvalue
Log2 fold change
b
-log10 Adj.Pvalue
Log2 fold change
c
-log10 Adj.Pvalue
Log2 fold change
d
-log10 Adj.Pvalue
Log2 fold change
e
-log10 Adj.Pvalue
Log2 fold change
f
-log10 Adj.Pvalue
Log2 fold change

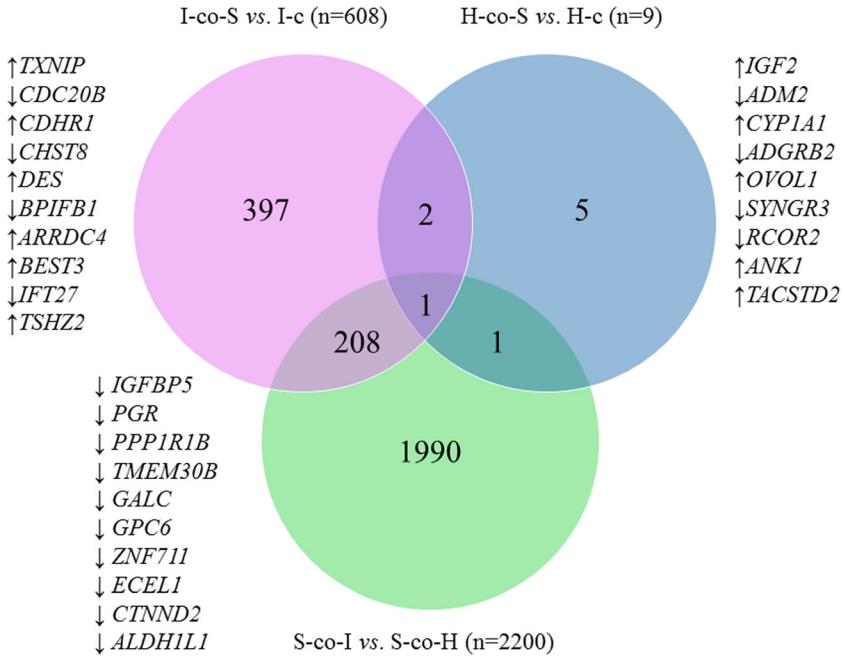

Fig. 4 Venn diagram representing differentially expressed genes among the following pairwise comparisons: (pink) Ishikawa substrates co-cultured with JEG-3 spheroids (I-co-S) vs. Ishikawa control (I-c), top 10 differentially expressed genes of this comparison ranked by absolute log2FC listed on the left; (blue) HEC-1-A substrates co-cultured with JEG-3 spheroids (H-co-S) vs. HEC-1-A control (H-c), all nine genes included in this comparison ranked by absolute log2FC listed on the right; and (green) JEG-3 spheroids co-cultured with Ishikawa substrates (S-co-I) vs. JEG-3 spheroids co-cultured with HEC-1-A substrates (S-co-H), top 10 differentially expressed genes of this comparison ranked by absolute log2FC listed on the left. The arrows show the direction of gene expression changes (↑ = upregulated, ↓ = downregulated)

Enrichment analysis of the trophoblast spheroids

The GSEA of the trophoblast spheroids showed involvement of a greater number of pathways than those detected in the epithelial compartments. In the S-co-I vs. S-co-H comparison, pathways overrepresented in S-co-I suggested increased tissue morphogenesis and organogenesis (e.g., cardiac muscle cell apoptotic process, middle ear morphogenesis, and regulation of organ formation), cell differentiation and development (e.g., peripheral nervous system neuron development, regulation of stem cell differentiation and anterior/posterior axis specification, embryo), angiogenesis (e.g., positive regulation of blood vessel endothelial cell migration, hypoxia, and angiogenesis), cell signaling (e.g., calcium-mediated signaling using intracellular calcium source, regulation of insulin-like growth factor receptor signaling pathway, and Kras signaling) as well as tissue remodeling (e.g., blastoderm segmentation and epithelial to mesenchymal transition) (Table 4). By contrast, the pathways overrepresented in S-co-H included cell proliferation and cell cycle regulation (e.g., DNA replication initiation, signal transduction involved in cell cycle checkpoint, and Myc targets), protein metabolism (e.g., tRNA processing and tRNA metabolic process), and immune response

Table 1 Biological pathways overrepresented in Ishikawa epithelial substrate after co-culture with JEG-3 spheroids vs. Ishikawa control using GOBP and Broad Hallmarks annotations

Annotation terms	Genes (*n*)	NES	FDR
Biological processes (GOBP)			
Mitotic spindle organization	38	1.91	0.098
Sister chromatid segregation	55	1.90	0.083
Mitotic sister chromatid segregation	52	1.88	0.079
Spindle organization	86	1.87	0.084
Rhodopsin mediated signaling pathway	34	1.85	0.090
Broad hallmarks			
E2F targets	196	1.87	0.003
G2M checkpoint	194	1.62	0.032
Allograft rejection	188	1.58	0.033
Apoptosis	158	1.52	0.044

NES normalized enrichment score, *FDR* false discovery rate

Table 2 Biological pathways overrepresented in HEC-1-A epithelial substrate after co-culture with JEG-3 spheroids vs. HEC-1-A control using GOBP and Broad Hallmarks annotations

Annotation terms	Genes (*n*)	NES	FDR
Biological processes (GOBP)			
Regulation of amino acid transport	18	1.94	0.028

NES normalized enrichment score, *FDR* false discovery rate

Table 3 Biological pathways overrepresented in the statistically significant gene expression pattern "upregulated in I-co-S vs. I-c and downregulated or unchanged in H-co-S vs. H-c" according to the hypergeometric test using GOBP and Broad Hallmarks annotations

Annotation terms	Genes (*n*)	Genes in the intersection (*n*)	Adj *p*-value	Genes in the intersection
Biological processes (GOBP)				
Nuclear division	346	32	0.00	*AURKB*, *BUB1*, *BUB1B*, *CAV2*, *CCNA2*, *CCNB2*, *CDC25C*, *CDCA2*, *CDCA5*, *CDCA8*, *CENPE*, *CENPW*, *CHEK2*, *CIT*, *DLGAP5*, *ERCC6L*, *INCENP*, *KIF11*, *KIF23*, *KIF2C*, *KIFC1*, *MAD2L1*, *NDC80*, *NUSAP1*, *PBK*, *PLK1*, *PSRC1*, *PTTG1*, *SPC24*, *SPC25*, *TTK*, *VRK1*
Mitosis	346	32	0.00	*AURKB*, *BUB1*, *BUB1B*, *CAV2*, *CCNA2*, *CCNB2*, *CDC25C*, *CDCA2*, *CDCA5*, *CDCA8*, *CENPE*, *CENPW*, *CHEK2*, *CIT*, *DLGAP5*, *ERCC6L*, *INCENP*, *KIF11*, *KIF23*, *KIF2C*, *KIFC1*, *MAD2L1*, *NDC80*, *NUSAP1*, *PBK*, *PLK1*, *PSRC1*, *PTTG1*, *SPC24*, *SPC25*, *TTK*, *VRK1*
Organelle fission	373	33	0.00	*AURKB*, *BUB1*, *BUB1B*, *CAV2*, *CCNA2*, *CCNB2*, *CDC25C*, *CDCA2*, *CDCA5*, *CDCA8*, *CENPE*, *CENPW*, *CHEK2*, *CIT*, *DLGAP5*, *ERCC6L*, *INCENP*, *KIF11*, *KIF23*, *KIF2C*, *KIFC1*, *MAD2L1*, *MTFR2*, *NDC80*, *NUSAP1*, *PBK*, *PLK1*, *PSRC1*, *PTTG1*, *SPC24*, *SPC25*, *TTK*, *VRK1*
Chromosome segregation	152	19	0.00	*AURKB*, *BUB1*, *CDCA5*, *CENPE*, *CENPW*, *CIT*, *DLGAP5*, *ECT2*, *HJURP*, *INCENP*, *KIF2C*, *KIFC1*, *MAD2L1*, *NDC80*, *NUSAP1*, *PLK1*, *PSRC1*, *PTTG1*, *SPC25*
Mitotic cell cycle	816	45	0.00	*AURKB*, *BUB1*, *BUB1B*, *CAV2*, *CCNA2*, *CCNB2*, *CDC25C*, *CDCA2*, *CDCA5*, *CDCA8*, *CDKN3*, *CENPE*, *CENPI*, *CENPW*, *CEP152*, *CHEK2*, *CIT*, *DLGAP5*, *ERCC6L*, *GINS4*, *ID2*, *INCENP*, *IQGAP3*, *KIF11*, *KIF20A*, *KIF23*, *KIF2C*, *KIFC1*, *LMNA*, *MAD2L1*, *NDC80*, *NUSAP1*, *PBK*, *PIM1*, *PLK1*, *PLK2*, *PSRC1*, *PTTG1*, *SPC24*, *SPC25*, *TTK*, *TUBB4A*, *TUBG2*, *USH1C*, *VRK1*
Mitotic spindle organization	39	9	0.00	*AURKB*, *CHEK2*, *KIF11*, *KIF23*, *NDC80*, *PLK2*, *PSRC1*, *SPC25*, *TTK*
Mitotic sister chromatid segregation	53	10	0.00	*CDCA5*, *CENPE*, *CIT*, *DLGAP5*, *KIFC1*, *MAD2L1*, *NDC80*, *NUSAP1*, *PLK1*, *PSRC1*
Sister chromatid segregation	56	10	0.00	*CDCA5*, *CENPE*, *CIT*, *DLGAP5*, *KIFC1*, *MAD2L1*, *NDC80*, *NUSAP1*, *PLK1*, *PSRC1*
Cell division	494	31	0,00	*AURKB*, *BUB1*, *BUB1B*, *CCNA2*, *CCNB2*, *CDC25C*, *CDCA2*, *CDCA5*, *CDCA8*, *CENPE*, *CENPW*, *CHEK2*, *CIT*, *ECT2*, *ERCC6L*, *INCENP*, *KIF11*, *KIF20A*, *KIF23*, *KIF2C*, *KIFC1*, *MAD2L1*, *NDC80*, *NUSAP1*, *PLK1*, *PSRC1*, *PTTG1*, *SPC24*, *SPC25*, *TXNIP*, *VRK1*
Spindle organization	88	11	0.00	*AURKB*, *BUB1B*, *CHEK2*, *KIF11*, *KIF23*, *NDC80*, *PLK2*, *PSRC1*, *SPC25*, *TACC3*, *TTK*
Cell cycle process	1117	49	0.01	*AURKB*, *BUB1*, *BUB1B*, *CAV2*, *CCNA2*, *CCNB2*, *CDC25C*, *CDCA2*, *CDCA5*, *CDCA8*, *CDKN3*, *CENPE*, *CENPW*, *CEP152*, *CGREF1*, *CHEK2*, *CIT*, *DLGAP5*, *ECT2*, *ERCC6L*, *EXO1*, *ID2*, *INCENP*, *IQGAP3*, *KIF11*, *KIF20A*, *KIF23*, *KIF2C*, *KIFC1*, *LMNA*, *MAD2L1*, *MKI67*, *NDC80*, *NUSAP1*, *PBK*, *PIM1*, *PLK1*, *PLK2*, *PSRC1*, *PTTG1*, *SPC24*, *SPC25*, *TACC3*, *TRIP13*, *TTK*, *TUBB4A*, *TUBG2*, *USH1C*, *VRK1*
Microtubule cytoskeleton organization	297	20	0.01	*AURKB*, *BUB1B*, *CAPN6*, *CEP152*, *CHEK2*, *ECT2*, *KIF11*, *KIF20A*, *KIF23*, *KIF2C*, *LMNA*, *NDC80*, *NUSAP1*, *PLK1*, *PLK2*, *PSRC1*, *SPC25*, *TACC3*, *TTK*, *TUBG2*
Microtubule-based process	456	26	0.01	*AP3B2*, *AURKB*, *BUB1B*, *CAPN6*, *CENPE*, *CEP152*, *CHEK2*, *DLGAP5*, *DNHD1*, *ECT2*, *KIF11*, *KIF20A*, *KIF23*, *KIF2C*, *KIFC1*, *LMNA*, *NDC80*, *NUSAP1*, *PLK1*, *PLK2*, *PSRC1*, *SPC25*, *TACC3*, *TTK*, *TUBB4A*, *TUBG2*
Metaphase/anaphase transition of mitotic cell cycle	43	7	0.02	*BUB1*, *BUB1B*, *CIT*, *DLGAP5*, *MAD2L1*, *PLK1*, *TTK*
Metaphase/anaphase transition of cell cycle	43	7	0.02	*BUB1*, *BUB1B*, *CIT*, *DLGAP5*, *MAD2L1*, *PLK1*, *TTK*
Cholesterol biosynthetic process	44	7	0.02	*FDFT1*, *FDPS*, *HMGCS1*, *IDI1*, *INSIG1*, *MSMO1*, *MVD*
Cell cycle	1464	57	0.03	*AURKB*, *BUB1*, *BUB1B*, *CAV2*, *CCNA2*, *CCNB2*, *CDC25C*, *CDCA2*, *CDCA5*, *CDCA8*, *CDKN3*, *CENPE*, *CENPI*, *CENPW*, *CEP152*, *CGREF1*, *CHEK2*, *CIT*, *DLGAP5*, *ECT2*, *ERCC6L*, *EXO1*, *FANCI*, *GINS4*, *HJURP*, *ID2*, *ID3*, *INCENP*, *IQGAP3*, *KIF11*, *KIF20A*, *KIF23*, *KIF2C*, *KIFC1*, *LMNA*, *MAD2L1*, *MKI67*, *NDC80*, *NUSAP1*,

Table 3 (continued)

Annotation terms	Genes (*n*)	Genes in the intersection (*n*)	Adj *p*-value	Genes in the intersection
				PBK PIM1, *PLK1*, *PLK2*, *PSRC1*, *PTTG1*, *RASSF2*, *RASSF4*, *SPC24*, *SPC25*, *TACC3*, *TRIP13*, *TTK*, *TUBB4A*, *TUBG2*, *TXNIP*, *USH1C*, *VRK1*
Sterol biosynthetic process	50	7	0.04	*FDFT1*, *FDPS*, *HMGCS1*, *IDI1*, *INSIG1*, *MSMO1*, *MVD*
Broad Hallmarks				
E2F_targets	200	23	0.00	*AURKB*, *BUB1B*, *CCNB2*, *CDCA8*, *CDKN3*, *CENPE*, *CHEK2*, *CIT*, *DIAPH3*, *DLGAP5*, *GINS4*, *KIF2C*, *MAD2L1*, *MKI67*, *MXD3*, *PLK1*, *PTTG1*, *RAD51AP1*, *SPC24*, *SPC25*, *TACC3*, *TK1*, *TRIP13*
G2M_checkpoint	200	22	0.00	*AURKB*, *BCL3*, *BUB1*, *CCNA2*, *CCNB2*, *CDKN3*, *CENPE*, *EXO1*, *INCENP*, *KIF11*, *KIF23*, *KIF2C*, *MAD2L1*, *MKI67*, *NDC80*, *NUSAP1*, *PBK*, *PLK1*, *POLQ*, *PTTG1*, *TACC3*, *TTK*
Mitotic_spindle	200	14	0.00	*BUB1*, *CCNB2*, *CENPE*, *DLGAP5*, *ECT2*, *EPB41L2*, *INCENP*, *KIF11*, *KIF23*, *KIF2C*, *NDC80*, *NUSAP1*, *PLK1*, *TTK*
Cholesterol_homeostasis	75	8	0.00	*ACSS2*, *FDFT1*, *FDPS*, *HMGCS1*, *IDI1*, *MVD*, *PPARG*, *SCD*

regulation (e.g., response to interferon alpha and interleukin-6 biosynthetic process) (Table 5).

RNA-seq validation

We used qPCR for validating the RNA-seq results of nine genes: *TMEM255A*, *EREG*, *SPDYC*, *CYP19A1*, *CASC1*, *PROM1*, *TGFA*, *CDC20B*, and *HPRT1*. In accordance with the RNA-seq, qPCR results confirmed upregulation of *EREG* (H-c vs. I-c), *SPDYC* (I-co-S vs. I-c), *PROM1* (S-co-I vs. S-c), and *TGFA* (S-co-I vs. S-c), downregulation of *TMEM255A* (H-c vs. I-c), *CYP19A1* (S-co-H vs. S-c), *CASC1* (S-co-I vs. S-co-H), and *CDC20B* (I-co-S vs. I-c) and similar levels of *HPRT1* (H-c vs. I-c) (Fig. 5).

Discussion

To our knowledge, this is the first study to analyze transcriptional dynamics of human implantation in a compartment-specific manner. In our in vitro model, transcriptional changes in both the embryo and endometrial epithelium proxies were dependent on endometrial receptivity, confirming that endometrium-driven molecular signals during attachment mediate embryo implantation.

Substrate response to embryo attachment

Our system successfully modeled known features of substrate response to contact with the trophoblast. As expected due to their different origins, the differences in the transcriptomic profiles of Ishikawa vs. HEC-1-A were numerous, as was their transcriptional response to co-culture with spheroids. Our datasets included genes previously related with implantation, such as *SPP1* (secreted phosphoprotein 1, which encodes the ECM component osteopontin), *OLFM2* (which encodes the ECM protein olfactomedin-2), and members of the Wnt signaling pathway (e.g., *WNT11*, *FZD8*, and *KREMEN2*) [22, 38–44]. In accordance with the role of cell adhesion and ECM proteins in the trophectoderm-epithelium interaction established in the literature [45–48], our results highlighted important transcriptional differences of genes involved in these processes, including cadherins (e.g., *PCDHA11*, *PCDHA12*, *CDH2*, and *CDHR1*), claudins (e.g., *CLDN16*), collagens (e.g., *COL9A3* and *COL5A1*), glycoproteins (e.g., *TNXB*), and metallopeptidases (e.g., *ADAM32*). In addition, the receptive epithelium responded to the trophoblast challenge by promoting pathways including mitotic spindle organization (suggesting increased cell division) and apoptosis, which is involved in the epithelial breaching by the embryo [49]. Of note, *C10orf10* and *G0S2*, which resulted differentially expressed among the substrates in our analysis, were previously suggested as transcriptomic biomarkers of endometrial receptivity [50].

Additionally, our model revealed emerging candidates in embryo attachment. *CDHR1* (cadherin-related family member 1) was strongly upregulated in Ishikawa cells after co-culture with spheroids and remained unchanged in HEC-1-A cells, compared to their respective non-co-cultured controls. The CDHR1 protein in endometrial fluid of healthy women has been suggested to be regulated by 17β-estradiol [51, 52]. Another gene family highlighted by our study is aquaporins. The expression levels *AQP3* and *AQP4* were upregulated in Ishikawa cells after the co-culture but not in HEC-1-A. Increased expression of *AQP3* has been associated with both epithelial cell migration and endometrial receptivity [53],

Table 4 Biological pathways overrepresented in trophoblast JEG-3 spheroids after co-culture with Ishikawa vs. HEC-1-A using GOBP and Broad Hallmarks annotations

Annotation terms	Genes (*n*)	NES	FDR
Biological processes (GOBP)			
Cardiac muscle cell apoptotic process	15	− 1.86	0.000
Striated muscle cell apoptotic process	18	− 1.84	0.002
Peripheral nervous system neuron development	13	− 1.82	0.003
Middle ear morphogenesis	24	− 1.80	0.006
Regulation of organ formation	36	− 1.78	0.012
Peripheral nervous system neuron differentiation	13	− 1.78	0.012
Anterior/posterior axis specification, embryo	15	− 1.77	0.012
Blastoderm segmentation	15	− 1.77	0.013
Tripartite regional subdivision	15	− 1.76	0.017
Regulation of cardiac muscle cell apoptotic process	12	− 1.76	0.017
Dicarboxylic acid catabolic process	15	− 1.75	0.018
Regulation of insulin-like growth factor receptor signaling pathway	19	− 1.75	0.018
Regulation of heart morphogenesis	24	− 1.75	0.019
Positive regulation of transforming growth factor beta receptor signaling pathway	22	− 1.74	0.021
Neuropeptide signaling pathway	56	− 1.74	0.022
Heart formation	14	− 1.74	0.023
Calcium-mediated signaling using intracellular calcium source	11	− 1.73	0.025
Regulation of fibroblast growth factor receptor signaling pathway	25	− 1.73	0.025
Regulation of striated muscle cell apoptotic process	15	− 1.73	0.026
Cell surface receptor signaling pathway involved in heart development	23	− 1.71	0.035
Outflow tract morphogenesis	52	− 1.69	0.056
Anterior/posterior axis specification	41	− 1.69	0.062
Cartilage development involved in endochondral bone morphogenesis	21	− 1.68	0.065
Eating behavior	22	− 1.68	0.064
Glutamate secretion	30	− 1.68	0.063
Regulation of cell proliferation involved in heart morphogenesis	15	− 1.68	0.062
Regulation of epithelial to mesenchymal transition	42	− 1.68	0.061
Face development	39	− 1.68	0.060
Embryonic cranial skeleton morphogenesis	38	− 1.67	0.066
Cell proliferation involved in heart morphogenesis	15	− 1.67	0.065
Insulin-like growth factor receptor signaling pathway	32	− 1.67	0.065
Positive regulation of blood vessel endothelial cell migration	21	− 1.67	0.064
Clathrin coat assembly	12	− 1.66	0.080
Embryonic skeletal system development	111	− 1.66	0.079
Regulation of stem cell differentiation	74	− 1.66	0.085
Embryonic skeletal system morphogenesis	84	− 1.65	0.088
Proximal/distal pattern formation	30	− 1.65	0.087
Negative regulation of striated muscle cell apoptotic process	12	− 1.65	0.099
Broad Hallmarks			
Hypoxia	194	− 1.51	0.090
Epithelial mesenchymal transition	195	− 1.46	0.082
Kras signaling dn	181	− 1.43	0.095
Angiogenesis	35	− 1.42	0.075

NES normalized enrichment score, *FDR* false discovery rate

while deficiency of *AQP4* leads to female subfertility in mice [54]. Other genes upregulated in Ishikawa cells upon trophoblast challenge were desmin (*DES*), adrenomedullin (*ADM*), and intermidin (*ADM2*). DES has been related to

Table 5 Biological pathways overrepresented in trophoblast JEG-3 spheroids after co-culture with HEC-1-A vs. Ishikawa using GOBP and Broad Hallmarks annotations

Annotation terms	Genes (*n*)	NES	FDR
Biological processes (GOBP)			
Detection of chemical stimulus involved in sensory perception of smell	21	2.32	0.002
Chromosome localization	22	2.26	0.003
Establishment of chromosome localization	21	2.20	0.007
tRNA processing	78	2.16	0.012
tRNA metabolic process	124	2.14	0.013
Metaphase plate congression	17	2.07	0.033
DNA strand elongation involved in DNA replication	33	2.07	0.031
Sensory perception of smell	43	2.06	0.029
Positive regulation of ubiquitin-protein ligase activity involved in mitotic cell cycle	72	2.04	0.035
Mitotic metaphase plate congression	13	2.04	0.033
Sister chromatid segregation	55	2.01	0.046
Negative regulation of ubiquitin-protein ligase activity involved in mitotic cell cycle	67	1.99	0.051
Anaphase-promoting complex-dependent proteasomal ubiquitin-dependent protein catabolic process	83	1.99	0.051
Mitotic sister chromatid segregation	52	1.97	0.058
Regulation of ubiquitin-protein ligase activity involved in mitotic cell cycle	78	1.96	0.061
Mitotic nuclear envelope disassembly	36	1.95	0.063
Response to interferon alpha	16	1.95	0.059
Cell cycle DNA replication	33	1.94	0.063
Histone exchange	24	1.94	0.060
Actin nucleation	13	1.94	0.058
ATP-dependent chromatin remodeling	30	1.92	0.067
DNA strand elongation	36	1.92	0.065
Detection of chemical stimulus involved in sensory perception	44	1.92	0.064
Positive regulation of ligase activity	86	1.90	0.078
ncRNA processing	206	1.89	0.085
DNA replication initiation	29	1.88	0.082
Interleukin-6 biosynthetic process	18	1.88	0.081
Negative regulation of ubiquitin-protein ligase activity	72	1.87	0.089
Negative regulation of ligase activity	72	1.87	0.087
Signal transduction involved in cell cycle checkpoint	66	1.85	0.098
Positive regulation of ubiquitin-protein ligase activity	82	1.85	0.098
Regulation of interleukin-6 biosynthetic process	16	1.84	0.097
ncRNA metabolic process	292	1.84	0.097
Nuclear envelope disassembly	38	1.83	0.098
Broad Hallmarks			
E2F targets	196	2.79	0.000
G2M checkpoint	194	2.72	0.000
Myc targets v1	196	2.39	0.000
Myc targets v2	58	1.89	0.000
Interferon alpha response	93	1.63	0.013

NES normalized enrichment score, *FDR* false discovery rate

decidualization and implantation in rodents [55]. *ADM*, which encodes for an endocrine peptide, has been linked to fertility in female mice; reduced expression levels of *ADM* impaired endometrial receptivity, and the administration of ADM prior to embryo transfer improved fertility by promoting pinopode formation [56–58]. In humans, a role for ADM in zygote transport in tubal ectopic pregnancies has been suggested [59]. The related protein

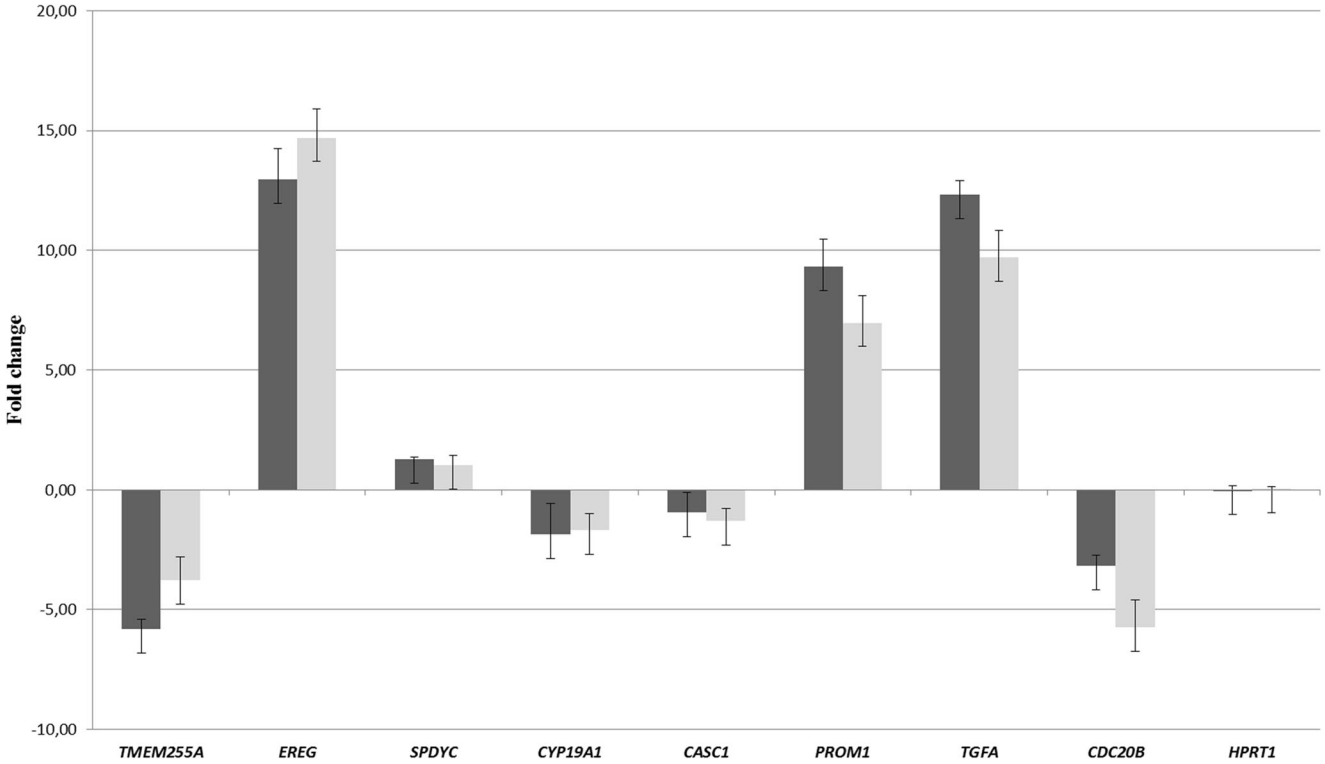

Fig. 5 RNA-seq validation by qPCR. Dark gray bars represent the differences in gene expression levels among samples (pairwise comparisons) by qPCR, and light gray bars represent the differences in gene expression levels among samples (pairwise comparisons) by RNA-seq. The genes and samples tested were: *TMEM255A* (H-c vs. I-c), *EREG* (H-c vs. I-c), *SPDYC* (I-co-S vs. I-c), *CYP19A1*(S-co-H vs. S-c), *CASC1* (S-co-I vs. S-co-H), *PROM1* (S-co-I vs. S-c), *TGFA* (S-co-I vs. S-c), *CDC20B* (I-co-S vs. I-c), and *HPRT1* (H-c vs. I-c). Error bars represent variability between sample triplicates from the original experimental sets

adrenomedullin 2 (also known as intermedin) has been associated with embryo implantation and placental growth [60]. The role of these genes in the trophoblast-epithelium interaction remains to be investigated.

Trophoblast response to attachment on epithelial substrates

Our model allowed us to examine the transcriptional response of the trophoblast to receptive or non-receptive substrates. Several trophoblast genes related with cell adhesion and ECM (*CD44*, *CTNND2*, *THBS1)* underwent upregulation upon co-culture of spheroids with Ishikawa cells (compared to HEC-1A cells), confirming previous reports that these three genes are differentially expressed in embryos that do attach to Ishikawa substrates compared to those which do not firmly attach [48]. Other genes followed a similar expression pattern: *TRO* (trophinin, an adhesion molecule uniquely expressed by human trophoblastic cells) and ErbB4 (a member in the EGFR subfamily of receptor tyrosine kinases) have been proposed as markers of initial embryo attachment [61, 62]. Further, co-culture on Ishikawa cells also resulted in upregulation of *DPY19L2*, a transmembrane protein coding gene which was previously related to male infertility; *DPY19L2* deletions are causative of around 70% of globozoospermia cases [63, 64].

Attachment in our model is driven by the endometrial compartment

The lack of receptivity of HEC-1-A is well established in the literature [17, 65]. Our study results showed that this lack of receptivity is due to a general inability of this substrate to mount a transcriptional response to the presence of the trophoblast spheroid. Indeed, when co-cultured with spheroids, the number of genes differentially expressed in Ishikawa cells vs. HEC-1-A cells was 608 vs. 9 genes, respectively. In turn, the different transcriptional responses of the two substrates conditioned the transcriptional response of the trophoblast spheroids. The trophoblast spheroids differentially expressed 3986 vs. 1038 genes when co-cultured with receptive vs. minimally receptive substrate, respectively, with overrepresentation of important pathways for future embryo development and pregnancy (e.g., organogenesis, morphogenesis, and angiogenesis) after interaction with Ishikawa cells. It has been demonstrated that embryos are able to self-organize while attached to cell-free surfaces, in the absence of maternal stimuli [66–68].

These studies highlight the importance of embryo regulation during later stages of development. However, implantation in maternal tissue is, ultimately, essential for developmental progression. We focus on early stages of implantation, where the crosstalk between the embryo and the maternal endometrium is essential [4, 10, 22]. Maternal induction of trophoblast differentiation has recently been found to be an important regulatory mechanism of implantation; although the mechanistic details have not been elucidated, the invasion needed for successful implantation has been shown to be dependent on maternal juxtacrine signals during apposition and attachment [10]. Different endometrial transcriptomic signatures during the window of implantation have been associated with reproductive success or failure [69–71]; a defective transcriptional substrate response to the presence of the embryo could underlie those transcriptomic signatures and lead to implantation failures.

Thus, by using a relatively simple 2D co-culture system, we confirm that the behavior of trophoblast spheroids on receptive vs. minimally receptive epithelial substrates was consistent with the expected changes during implantation, as previously described in another model [5, 72], and identified several candidate genes for future study.

A strength of our study is a novel experimental design which uses FACS to isolate individual compartments, allowing us to analyze the transcriptional response of each compartment to the other after co-culture. Further, RNA samples were harvested from pools of 96-well plates where each well contained a single spheroid on a fixed area of substrate (keeping the substrate/spheroid ratio constant) and therefore lending reproducibility and robustness to our results. A number of studies have determined the transcriptional signature of the endometrium and its correlation with implantation and reproductive outcome [69, 70, 73, 74]. Our study highlights the significance of focusing not only on the endometrium per se, but on its ability to mount the correct transcriptional response upon interaction with the embryo.

The convenience of using an in vitro experimental approach entails limitations in our study. It has been confirmed that in vitro cell culture induces changes in the cell transcriptome, which limits the extrapolation of our study results [75]. Although broadly used in the literature to study implantation, JEG-3, Ishikawa, and HEC-1-A cell lines come from a carcinogenic origin and might not represent the physiological conditions of the implantation process [76]. Trophoblast spheroids lack communication between the inner cell mass and the trophectoderm, and they are committed cells from a later developmental stage; therefore, their response does not fully represent a viable real embryo. Nevertheless, the JEG-3 cell line present specific characteristics that resemble normal primary trophoblast cells, such as hCG production, glucose transport, and cell barrier integrity [77, 78]. The 3-D structure provides transcriptional profiles and secretory activities more similar to those from primary trophoblasts compared to 2-D cultures [79]. Of note, no hormones were used during cell culture (e.g., progesterone or estrogen), which could change expression levels of some transcripts [21, 80]. We chose a 48-h co-culture based on the morphological changes observed in our system and previous reports; different end points could give different results. These features in our experimental setup could explain that some genes we were expecting to find involved in attachment based on previous literature such as epithelial *MUC-1*, *LIF*, *HB-EGF*, and *HOXA10* as well as trophoblast *IL-1* and *MMP-9* [20, 81–85] were not detected in our analysis. Both Ishikawa and HEC-1-A cells express estrogen and progesterone receptors and are responsive to hormones in terms of gene expression [20, 21, 86, 87]. However, they do not reproduce the non-receptive to receptive phenotype change that epithelial cells undergo during the menstrual cycle under the influence of ovarian steroids. Therefore, hormonal supplementation is not likely to cause a great effect on gene expression in co-culture experiments [88].

The application of our methodological approach to primary epithelial and stromal cells obtained from patients will provide extended information about the mechanisms involved in implantation failure. In summary, our transcriptional results suggest that endometrial receptivity determines the degree of trophoblast response and drives attachment during human implantation.

Acknowledgements The authors wish to thank all members of the Basic Laboratory from Clínica EUGIN, especially Montserrat Barragán and Anna Ferrer, for critical discussion; José Buratini from Sao Paulo State University (Brasil) for critical revision of the manuscript; Camille Stephan Otto from the Biostatistics/Bioinformatics facility of the Institute for Research in Biomedicine (Barcelona) for bioinformatics analysis; Charles Pineau, Natalie Melaine, and Emmanuelle Com from Proteomics Core Facility Biogenouest (Rennes) for assistance with data analysis; and Prof. Daniel Grinberg from Universitat de Barcelona for technical support.

Author's contribution Paula Vergaro: experimental execution, study design, data analysis, and manuscript preparation. Gustavo Tiscornia: study design and supervision, data analysis, manuscript edition, and expert knowledge. Amelia Rodríguez: study supervision. Josep Santaló: study supervision, expert knowledge, and manuscript edition. Rita Vassena: study design and supervision, expert knowledge, and manuscript edition.

Funding This work was supported by intramural funding of Clínica EUGIN and by the Secretary for Universities and Research of the Ministry of Economy and Knowledge of the Government of Catalonia (GENCAT 2015 DI 050).

Compliance with ethical standards

Conflict of interest The authors declare that they have no conflict of interest.

References

1. Sharkey AM, Macklon NS. The science of implantation emerges blinking into the light. Reprod BioMed Online. 2013;27(5):453–60. https://doi.org/10.1016/j.rbmo.2013.08.005.
2. Hannan NJ, Jones RL, White CA, Salamonsen LA. The chemokines, CX3CL1, CCL14, and CCL4, promote human trophoblast migration at the feto-maternal interface. Biol Reprod. 2006;74(5):896–904. https://doi.org/10.1095/biolreprod.105.045518.
3. Hannan NJ, Paiva P, Meehan KL, Rombauts LJ, Gardner DK, Salamonsen LA. Analysis of fertility-related soluble mediators in human uterine fluid identifies VEGF as a key regulator of embryo implantation. Endocrinology. 2011;152(12):4948–56. https://doi.org/10.1210/en.2011-1248.
4. Greening DW, Nguyen HP, Elgass K, Simpson RJ, Salamonsen LA. Human endometrial exosomes contain hormone-specific cargo modulating trophoblast adhesive capacity: insights into endometrial-embryo interactions. Biol Reprod. 2016;94(2):38. https://doi.org/10.1095/biolreprod.115.134890.
5. Wang H, Dey SK. Roadmap to embryo implantation: clues from mouse models. Nat Rev Genet. 2006;7(3):185–99. https://doi.org/10.1038/nrg1808.
6. Teklenburg G, Salker M, Molokhia M, Lavery S, Trew G, Aojanepong T, et al. Natural selection of human embryos: decidualizing endometrial stromal cells serve as sensors of embryo quality upon implantation. PLoS One. 2010;5(4):e10258. https://doi.org/10.1371/journal.pone.0010258.
7. Weimar CH, Kavelaars A, Brosens JJ, Gellersen B, de Vreeden-Elbertse JM, Heijnen CJ, et al. Endometrial stromal cells of women with recurrent miscarriage fail to discriminate between high- and low-quality human embryos. PLoS One. 2012;7(7):e41424. https://doi.org/10.1371/journal.pone.0041424.
8. Salker MS, Nautiyal J, Steel JH, Webster Z, Sucurovic S, Nicou M, et al. Disordered IL-33/ST2 activation in decidualizing stromal cells prolongs uterine receptivity in women with recurrent pregnancy loss. PLoS One. 2012;7(12):e52252. https://doi.org/10.1371/journal.pone.0052252.
9. Brighton PJ, Maruyama Y, Fishwick K, Vrljicak P, Tewary S, Fujihara R, Muter J, Lucas ES, Yamada T, Woods L, Lucciola R, Hou Lee Y, Takeda S, Ott S, Hemberger M, Quenby S, Brosens JJ Clearance of senescent decidual cells by uterine natural killer cells in cycling human endometrium. eLife. 2017;6. doi:https://doi.org/10.7554/eLife.31274.
10. Ruane PT, Berneau SC, Koeck R, Watts J, Kimber SJ, Brison DR, et al. Apposition to endometrial epithelial cells activates mouse blastocysts for implantation. Mol Hum Reprod. 2017;23(9):617–27. https://doi.org/10.1093/molehr/gax043.
11. Polanski LT, Baumgarten MN, Quenby S, Brosens J, Campbell BK, Raine-Fenning NJ. What exactly do we mean by 'recurrent implantation failure'? A systematic review and opinion. Reprod BioMed Online. 2014;28(4):409–23. https://doi.org/10.1016/j.rbmo.2013.12.006.
12. Miller PB, Parnell BA, Bushnell G, Tallman N, Forstein DA, Higdon HL 3rd, et al. Endometrial receptivity defects during IVF cycles with and without letrozole. Hum Reprod. 2012;27(3):881–8. https://doi.org/10.1093/humrep/der452.
13. Namiki T, Ito J, Kashiwazaki N. Molecular mechanisms of embryonic implantation in mammals: lessons from the gene manipulation of mice. RMB. 2018;17(4):331–42. https://doi.org/10.1002/rmb2.12103.
14. Melford SE, Taylor AH, Konje JC. Of mice and (wo)men: factors influencing successful implantation including endocannabinoids. Hum Reprod Update. 2014;20(3):415–28. https://doi.org/10.1093/humupd/dmt060.
15. Cha J, Sun X, Dey SK. Mechanisms of implantation: strategies for successful pregnancy. Nat Med. 2012;18(12):1754–67. https://doi.org/10.1038/nm.3012.
16. Aplin JD, Ruane PT. Embryo-epithelium interactions during implantation at a glance. J Cell Sci. 2017;130(1):15–22. https://doi.org/10.1242/jcs.175943.
17. Dominguez F, Avila S, Cervero A, Martin J, Pellicer A, Castrillo JL, et al. A combined approach for gene discovery identifies insulin-like growth factor-binding protein-related protein 1 as a new gene implicated in human endometrial receptivity. J Clin Endocrinol Metab. 2003;88(4):1849–57. https://doi.org/10.1210/jc.2002-020724.
18. Heneweer C, Schmidt M, Denker HW, Thie M. Molecular mechanisms in uterine epithelium during trophoblast binding: the role of small GTPase RhoA in human uterine Ishikawa cells. J Exp Clin Assist Reprod. 2005;2(1):4. https://doi.org/10.1186/1743-1050-2-4.
19. Uchida H, Maruyama T, Ohta K, Ono M, Arase T, Kagami M, et al. Histone deacetylase inhibitor-induced glycodelin enhances the initial step of implantation. Hum Reprod. 2007;22(10):2615–22. https://doi.org/10.1093/humrep/dem263.
20. Singh H, Nardo L, Kimber SJ, Aplin JD. Early stages of implantation as revealed by an in vitro model. Reproduction. 2010;139(5):905–14. https://doi.org/10.1530/REP-09-0271.
21. Tamm-Rosenstein K, Simm J, Suhorutshenko M, Salumets A, Metsis M. Changes in the transcriptome of the human endometrial Ishikawa cancer cell line induced by estrogen, progesterone, tamoxifen, and mifepristone (RU486) as detected by RNA-sequencing. PLoS One. 2013;8(7):e68907. https://doi.org/10.1371/journal.pone.0068907.
22. Kang YJ, Forbes K, Carver J, Aplin JD. The role of the osteopontin-integrin alphavbeta3 interaction at implantation: functional analysis using three different in vitro models. Hum Reprod. 2014;29(4):739–49. https://doi.org/10.1093/humrep/det433.
23. Berger C, Boggavarapu NR, Menezes J, Lalitkumar PG, Gemzell-Danielsson K. Effects of ulipristal acetate on human embryo attachment and endometrial cell gene expression in an in vitro co-culture system. Hum Reprod. 2015;30(4):800–11. https://doi.org/10.1093/humrep/dev030.
24. Boggavarapu NR, Berger C, von Grothusen C, Menezes J, Gemzell-Danielsson K, Lalitkumar PG. Effects of low doses of mifepristone on human embryo implantation process in a three-dimensional human endometrial in vitro co-culture system. Contraception. 2016;94(2):143–51. https://doi.org/10.1016/j.contraception.2016.03.009.
25. Carver J, Martin K, Spyropoulou I, Barlow D, Sargent I, Mardon H. An in-vitro model for stromal invasion during implantation of the human blastocyst. Hum Reprod. 2003;18(2):283–90.
26. Tiscornia G, Singer O, Verma IM. Production and purification of lentiviral vectors. Nat Protoc. 2006;1(1):241–5. https://doi.org/10.1038/nprot.2006.37.
27. Dobin A, Davis CA, Schlesinger F, Drenkow J, Zaleski C, Jha S, et al. STAR: ultrafast universal RNA-seq aligner. Bioinformatics. 2013;29(1):15–21. https://doi.org/10.1093/bioinformatics/bts635.
28. Liao Y, Smyth GK, Shi W. The subread aligner: fast, accurate and scalable read mapping by seed-and-vote. Nucleic Acids Res. 2013;41(10):e108. https://doi.org/10.1093/nar/gkt214.
29. Smedley D, Haider S, Durinck S, Pandini L, Provero P, Allen J, et al. The BioMart community portal: an innovative alternative to large, centralized data repositories. Nucleic Acids Res. 2015;43(W1):W589–98. https://doi.org/10.1093/nar/gkv350.
30. Love MI, Huber W, Anders S. Moderated estimation of fold change and dispersion for RNA-seq data with DESeq2. Genome Biol. 2014;15(12):550. https://doi.org/10.1186/s13059-014-0550-8.
31. Subramanian A, Tamayo P, Mootha VK, Mukherjee S, Ebert BL, Gillette MA, et al. Gene set enrichment analysis: a knowledge-

based approach for interpreting genome-wide expression profiles. Proc Natl Acad Sci U S A. 2005;102(43):15545–50. https://doi.org/10.1073/pnas.0506580102.
32. Ashburner M, Ball CA, Blake JA, Botstein D, Butler H, Cherry JM, et al. Gene ontology: tool for the unification of biology. The Gene Ontology Consortium. Nat Gen. 2000;25(1):25–9. https://doi.org/10.1038/75556.
33. Morgan M FSaGR. Morgan M, Falcon S and Gentleman R (2017). GSEABase: Gene set enrichment data structures and methods. R package version 1.40.1. 2017.
34. Liberzon A, Birger C, Thorvaldsdottir H, Ghandi M, Mesirov JP, Tamayo P. The molecular signatures database (MSigDB) hallmark gene set collection. Cell Syst. 2015;1(6):417–25. https://doi.org/10.1016/j.cels.2015.12.004.
35. Liberzon A, Subramanian A, Pinchback R, Thorvaldsdottir H, Tamayo P, Mesirov JP. Molecular signatures database (MSigDB) 3.0. Bioinformatics. 2011;27(12):1739–40. https://doi.org/10.1093/bioinformatics/btr260.
36. Xie F, Sun G, Stiller JW, Zhang B. Genome-wide functional analysis of the cotton transcriptome by creating an integrated EST database. PLoS One. 2011;6(11):e26980. https://doi.org/10.1371/journal.pone.0026980.
37. Vandesompele J, De Preter K, Pattyn F, Poppe B, Van Roy N, De Paepe A, et al. Accurate normalization of real-time quantitative RT-PCR data by geometric averaging of multiple internal control genes. Genome Biol. 2002;3(7):RESEARCH0034.
38. Borthwick JM, Charnock-Jones DS, Tom BD, Hull ML, Teirney R, Phillips SC, et al. Determination of the transcript profile of human endometrium. Mol Hum Reprod. 2003;9(1):19–33.
39. White FJ, Burghardt RC, Hu J, Joyce MM, Spencer TE, Johnson GA. Secreted phosphoprotein 1 (osteopontin) is expressed by stromal macrophages in cyclic and pregnant endometrium of mice, but is induced by estrogen in luminal epithelium during conceptus attachment for implantation. Reproduction. 2006;132(6):919–29. https://doi.org/10.1530/REP-06-0068.
40. Quenby S, Anim-Somuah M, Kalumbi C, Farquharson R, Aplin JD. Different types of recurrent miscarriage are associated with varying patterns of adhesion molecule expression in endometrium. Reprod BioMed Online. 2007;14(2):224–34.
41. Kodithuwakku SP, Ng PY, Liu Y, Ng EH, Yeung WS, Ho PC, et al. Hormonal regulation of endometrial olfactomedin expression and its suppressive effect on spheroid attachment onto endometrial epithelial cells. Hum Reprod. 2011;26(1):167–75. https://doi.org/10.1093/humrep/deq298.
42. Tepekoy F, Akkoyunlu G, Demir R. The role of Wnt signaling members in the uterus and embryo during pre-implantation and implantation. J Assist Reprod Genet. 2015;32(3):337–46. https://doi.org/10.1007/s10815-014-0409-7.
43. Zhang Q, Yan J. Update of Wnt signaling in implantation and decidualization. RMB. 2016;15(2):95–105. https://doi.org/10.1007/s12522-015-0226-4.
44. Farah O, Biechele S, Rossant J, Dufort D. Porcupine-dependent Wnt activity within the uterine epithelium is essential for fertility. Biol Reprod. 2017;97(5):688–97. https://doi.org/10.1093/biolre/iox119.
45. Haouzi D, Dechaud H, Assou S, Monzo C, de Vos J, Hamamah S. Transcriptome analysis reveals dialogues between human trophectoderm and endometrial cells during the implantation period. Hum Reprod. 2011;26(6):1440–9. https://doi.org/10.1093/humrep/der075.
46. Singh H, Aplin JD. Endometrial apical glycoproteomic analysis reveals roles for cadherin 6, desmoglein-2 and plexin b2 in epithelial integrity. Mol Hum Reprod. 2015;21(1):81–94. https://doi.org/10.1093/molehr/gau087.
47. Altmae S, Reimand J, Hovatta O, Zhang P, Kere J, Laisk T, et al. Research resource: interactome of human embryo implantation: identification of gene expression pathways, regulation, and integrated regulatory networks. Mol Endocrinol. 2012;26(1):203–17. https://doi.org/10.1210/me.2011-1196.
48. Aberkane A, Essahib W, Spits C, De Paepe C, Sermon K, Adriaenssens T, et al. Expression of adhesion and extracellular matrix genes in human blastocysts upon attachment in a 2D co-culture system. Mol Hum Reprod. 2018;24(7):375–87. https://doi.org/10.1093/molehr/gay024.
49. Arase T, Uchida H, Kajitani T, Ono M, Tamaki K, Oda H, et al. The UDP-glucose receptor P2RY14 triggers innate mucosal immunity in the female reproductive tract by inducing IL-8. J Immunol. 2009;182(11):7074–84. https://doi.org/10.4049/jimmunol.0900001.
50. Altmae S, Koel M, Vosa U, Adler P, Suhorutsenko M, Laisk-Podar T, et al. Meta-signature of human endometrial receptivity: a meta-analysis and validation study of transcriptomic biomarkers. Sci Rep. 2017;7(1):10077. https://doi.org/10.1038/s41598-017-10098-3.
51. Chan C, Virtanen C, Winegarden NA, Colgan TJ, Brown TJ, Greenblatt EM. Discovery of biomarkers of endometrial receptivity through a minimally invasive approach: a validation study with implications for assisted reproduction. Fertil Steril. 2013;100(3):810–7. https://doi.org/10.1016/j.fertnstert.2013.04.047.
52. Humphreys GI, Ziegler YS, Nardulli AM. 17beta-estradiol modulates gene expression in the female mouse cerebral cortex. PLoS One. 2014;9(11):e111975. https://doi.org/10.1371/journal.pone.0111975.
53. Cui D, Sui L, Han X, Zhang M, Guo Z, Chen W, et al. Aquaporin-3 mediates ovarian steroid hormone-induced motility of endometrial epithelial cells. Hum Reprod. 2018;33(11):2060–73. https://doi.org/10.1093/humrep/dey290.
54. Sun XL, Zhang J, Fan Y, Ding JH, Sha JH, Hu G. Aquaporin-4 deficiency induces subfertility in female mice. Fertil Steril. 2009;92(5):1736–43. https://doi.org/10.1016/j.fertnstert.2008.07.1785.
55. Korgun ET, Cayli S, Asar M, Demir R. Distribution of laminin, vimentin and desmin in the rat uterus during initial stages of implantation. J Mol Histol. 2007;38(4):253–60. https://doi.org/10.1007/s10735-007-9095-4.
56. Li M, Yee D, Magnuson TR, Smithies O, Caron KM. Reduced maternal expression of adrenomedullin disrupts fertility, placentation, and fetal growth in mice. J Clin Invest. 2006;116(10):2653–62. https://doi.org/10.1172/JCI28462.
57. Li M, Wu Y, Caron KM. Haploinsufficiency for adrenomedullin reduces pinopodes and diminishes uterine receptivity in mice. Biol Reprod. 2008;79(6):1169–75. https://doi.org/10.1095/biolreprod.108.069336.
58. Matson BC, Pierce SL, Espenschied ST, Holle E, Sweatt IH, Davis ES, et al. Adrenomedullin improves fertility and promotes pinopodes and cell junctions in the peri-implantation endometrium. Biol Reprod. 2017;97(3):466–77. https://doi.org/10.1093/biolre/iox101.
59. Liao SB, Li HW, Ho JC, Yeung WS, Ng EH, Cheung AN, et al. Possible role of adrenomedullin in the pathogenesis of tubal ectopic pregnancy. J Clin Endocrinol Metab. 2012;97(6):2105–12. https://doi.org/10.1210/jc.2011-3290.
60. Havemann D, Balakrishnan M, Borahay M, et al. Intermedin/adrenomedullin 2 is associated with implantation and placentation via trophoblast invasion in human pregnancy. J Clin Endocrinol Metab. 2013;98(2):695–703. Published online 2013 Jan 21. https://doi.org/10.1210/jc.2012-2172.
61. Chobotova K, Spyropoulou I, Carver J, Manek S, Heath JK, Gullick WJ, et al. Heparin-binding epidermal growth factor and its receptor ErbB4 mediate implantation of the human blastocyst. Mech Dev. 2002;119(2):137–44.

62. Sugihara K, Sugiyama D, Byrne J, Wolf DP, Lowitz KP, Kobayashi Y, et al. Trophoblast cell activation by trophinin ligation is implicated in human embryo implantation. Proc Natl Acad Sci U S A. 2007;104(10):3799–804. https://doi.org/10.1073/pnas.0611516104.
63. Harbuz R, Zouari R, Pierre V, Ben Khelifa M, Kharouf M, Coutton C, et al. A recurrent deletion of DPY19L2 causes infertility in man by blocking sperm head elongation and acrosome formation. Am J Hum Genet. 2011;88(3):351–61. https://doi.org/10.1016/j.ajhg.2011.02.007.
64. Modarres P, Tanhaei S, Tavalaee M, Ghaedi K, Deemeh MR, Nasr-Esfahani MH. Assessment of DPY19L2 deletion in familial and non-familial individuals with globozoospermia and DPY19L2 genotyping. Int J Fertil Steril. 2016;10(2):196–207.
65. Tamm K, Room M, Salumets A, Metsis M. Genes targeted by the estrogen and progesterone receptors in the human endometrial cell lines HEC1A and RL95-2. Reprod Biol Endocrinol. 2009;7:150. https://doi.org/10.1186/1477-7827-7-150.
66. Harrison SE, Sozen B, Christodoulou N, Kyprianou C, Zernicka-Goetz M. Assembly of embryonic and extraembryonic stem cells to mimic embryogenesis in vitro. Science. 2017;356(6334):eaal1810. https://doi.org/10.1126/science.aal1810.
67. Shahbazi MN, Scialdone A, Skorupska N, Weberling A, Recher G, Zhu M, et al. Pluripotent state transitions coordinate morphogenesis in mouse and human embryos. Nature. 2017;552(7684):239–43. https://doi.org/10.1038/nature24675.
68. Sozen B, Amadei G, Cox A, Wang R, Na E, Czukiewska S, et al. Self-assembly of embryonic and two extra-embryonic stem cell types into gastrulating embryo-like structures. Nat Cell Biol. 2018;20(8):979–89. https://doi.org/10.1038/s41556-018-0147-7.
69. Koot YE, van Hooff SR, Boomsma CM, van Leenen D, Groot Koerkamp MJ, Goddijn M, et al. An endometrial gene expression signature accurately predicts recurrent implantation failure after IVF. Sci Rep. 2016;6:19411. https://doi.org/10.1038/srep19411.
70. Diaz-Gimeno P, Ruiz-Alonso M, Sebastian-Leon P, Pellicer A, Valbuena D, Simon C. Window of implantation transcriptomic stratification reveals different endometrial subsignatures associated with live birth and biochemical pregnancy. Fertil Steril. 2017;108(4):703–10 e3. https://doi.org/10.1016/j.fertnstert.2017.07.007.
71. Huang J, Qin H, Yang Y, Chen X, Zhang J, Laird S, et al. A comparison of transcriptomic profiles in endometrium during window of implantation between women with unexplained recurrent implantation failure and recurrent miscarriage. Reproduction. 2017;153(6):749–58. https://doi.org/10.1530/REP-16-0574.
72. Wang H, Pilla F, Anderson S, Martinez-Escribano S, Herrer I, Moreno-Moya JM, et al. A novel model of human implantation: 3D endometrium-like culture system to study attachment of human trophoblast (Jar) cell spheroids. Mol Hum Reprod. 2012;18(1):33–43. https://doi.org/10.1093/molehr/gar064.
73. Altmae S, Martinez-Conejero JA, Salumets A, Simon C, Horcajadas JA, Stavreus-Evers A. Endometrial gene expression analysis at the time of embryo implantation in women with unexplained infertility. Mol Hum Reprod. 2010;16(3):178–87. https://doi.org/10.1093/molehr/gap102.
74. Enciso M, Carrascosa JP, Sarasa J, Martinez-Ortiz PA, Munne S, Horcajadas JA, et al. Development of a new comprehensive and reliable endometrial receptivity map (ER map/ER grade) based on RT-qPCR gene expression analysis. Hum Reprod. 2018;33(2):220–8. https://doi.org/10.1093/humrep/dex370.
75. Krjutskov K, Katayama S, Saare M, Vera-Rodriguez M, Lubenets D, Samuel K, et al. Single-cell transcriptome analysis of endometrial tissue. Hum Reprod. 2016;31(4):844–53. https://doi.org/10.1093/humrep/dew008.
76. Hannan NJ, Paiva P, Dimitriadis E, Salamonsen LA. Models for study of human embryo implantation: choice of cell lines? Biol Reprod. 2010;82(2):235–45. https://doi.org/10.1095/biolreprod.109.077800.
77. Huang X, Luthi M, Ontsouka EC, Kallol S, Baumann MU, Surbek DV, et al. Establishment of a confluent monolayer model with human primary trophoblast cells: novel insights into placental glucose transport. Mol Hum Reprod. 2016;22(6):442–56. https://doi.org/10.1093/molehr/gaw018.
78. Rothbauer M, Patel N, Gondola H, Siwetz M, Huppertz B, Ertl P. A comparative study of five physiological key parameters between four different human trophoblast-derived cell lines. Sci Rep. 2017;7(1):5892. https://doi.org/10.1038/s41598-017-06364-z.
79. McConkey CA, Delorme-Axford E, Nickerson CA, Kim KS, Sadovsky Y, Boyle JP, et al. A three-dimensional culture system recapitulates placental syncytiotrophoblast development and microbial resistance. Sci Adv. 2016;2(3):e1501462. https://doi.org/10.1126/sciadv.1501462.
80. Dassen H, Punyadeera C, Kamps R, Klomp J, Dunselman G, Dijcks F, et al. Progesterone regulation of implantation-related genes: new insights into the role of oestrogen. Cell Mol Life Sci. 2007;64(7–8):1009–32. https://doi.org/10.1007/s00018-007-6553-9.
81. Paiva P, Menkhorst E, Salamonsen L, Dimitriadis E. Leukemia inhibitory factor and interleukin-11: critical regulators in the establishment of pregnancy. Cytokine Growth Factor Rev. 2009;20(4):319–28. https://doi.org/10.1016/j.cytogfr.2009.07.001.
82. Franasiak JM, Holoch KJ, Yuan L, Schammel DP, Young SL, Lessey BA. Prospective assessment of midsecretory endometrial leukemia inhibitor factor expression versus alphanubeta3 testing in women with unexplained infertility. Fertil Steril. 2014;101(6):1724–31. https://doi.org/10.1016/j.fertnstert.2014.02.027.
83. Lessey BA, Castelbaum AJ. Integrins and implantation in the human. Rev Endocr Metab Disord. 2002;3(2):107–17.
84. Hirota Y, Osuga Y, Hasegawa A, Kodama A, Tajima T, Hamasaki K, et al. Interleukin (IL)-1beta stimulates migration and survival of first-trimester villous cytotrophoblast cells through endometrial epithelial cell-derived IL-8. Endocrinology. 2009;150(1):350–6. https://doi.org/10.1210/en.2008-0264.
85. Plaks V, Rinkenberger J, Dai J, Flannery M, Sund M, Kanasaki K, et al. Matrix metalloproteinase-9 deficiency phenocopies features of preeclampsia and intrauterine growth restriction. Proc Natl Acad Sci U S A. 2013;110(27):11109–14. https://doi.org/10.1073/pnas.1309561110.
86. Kurarmoto H, Hamano M, Imai M. HEC-1 cells. Hum Cell. 2002;15(2):81–95. https://doi.org/10.1111/j.1749-0774.2002.tb00103.x.
87. Thie M, Denker HW. In vitro studies on endometrial adhesiveness for trophoblast: cellular dynamics in uterine epithelial cells. Cells Tissues Organs. 2002;172(3):237–52. https://doi.org/10.1159/000066963.
88. Rahimipour M, Salehnia M, Jafarabadi M. Morphological, ultrastructural, and molecular aspects of in vitro mouse embryo implantation on human endometrial mesenchymal stromal cells in the presence of steroid hormones as an implantation model. Cell J. 2018;20(3):369–76. https://doi.org/10.22074/cellj.2018.5221.